ARCHEOPS : Measurement of the CMB Power Spectrum on Small and Large Angular Scales and First Detection of Polarization of the Submillimetre Diffuse Galactic Dust Emission

Nicolas Ponthieu
On behalf of ARCHEOPS collaboration[a]
IAS, Université Paris–Sud, Bat. 121, F–91405 ORSAY, France
Nicolas.Ponthieu@ias.u-psud.fr

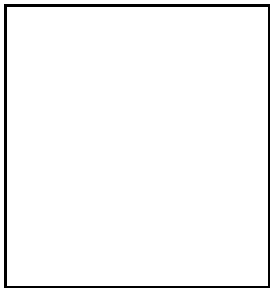

Abstract

ARCHEOPS is a balloon borne experiment designed to map the Cosmic Microwave Background (CMB) anisotropies over a large fraction of the sky ($\sim 30\%$) during a single arctic night flight, with a high angular resolution (~ 10 arcmin), and to study Galactic foregrounds radiation in the submillimetre domain. The channels at 143 GHz and 217 GHz are more dedicated to CMB studies, those at 545 GHz and 353 GHz are used for Galactic studies. The bolometers operating at 353 GHz are mounted in three polarization sensitive pairs. We briefly present the instrument, the results of the CMB power spectrum estimation, the constrain on cosmological parameters and report the first measurement of the submillimetre diffuse Galactic dust emission.

1 Introduction

The power spectrum of the temperature anisotropies of the Cosmic Microwave Background (CMB) has proved to be a powerful tool for constraining the cosmological parameters. Since the first detection of CMB anisotropy with COBE/DMR [40], a host of experiments have measured the spectrum down to sub–degree scales, but measurements at large angular scales have remained difficult, due to the large sky coverage required to access these modes. This difficulty was first overcome by ARCHEOPS in year 2002 [3] and contributed to improve the accuracy on the determination of the major cosmological parameters [4].

Whereas CMB *temperature* anisotropies have now been measured over most of the relevant angular scales (10 arcmin to 90 degrees[b]), CMB *polarization* is only in its experimental infancy. Theoretical predictions are rather tight for the polarization effect coming from the last scattering surface. Upper limits on polarization [27,15] are now superseded by detections by DASI [30] and WMAP [29] of the scalar mode E (for a review, see Carlstrom [12]). New results can be expected from various experiments, on ground or balloon borne, and later from PLANCK. The detection of tensor mode B, opens a unique window on the primordial Universe, but remains at an uncertain level and is even more challenging to detect, therefore requiring an even greater control of the systematics and foregrounds radiation.

[a] Includes scientists from Berkeley (USA), Caltech (Passadena, USA), Cardiff Univ. (UK), CESR (Toulouse, France), CSNSM (Orsay, France), CRTBT (Grenoble, France), IAS (Orsay, France), IAP (Paris, France), IROE (Firenze, Italy), JPL (Passadena, USA), LAL (Orsay, France), LAOG (Grenoble, France), Landau Institute (Moscow, Russia), LPSC (Grenoble, France), La Sapienza Univ. (Roma, Italy), LAOMP (Toulouse, France), Maynooth Univ. (Ireland), Minnesota Univ. (USA), PCC (Paris, France), Princeton (USA), SPP (France).

[b] See a comparison of different experiments in Benoît *et al* [7] and Bennett *et al* [2].

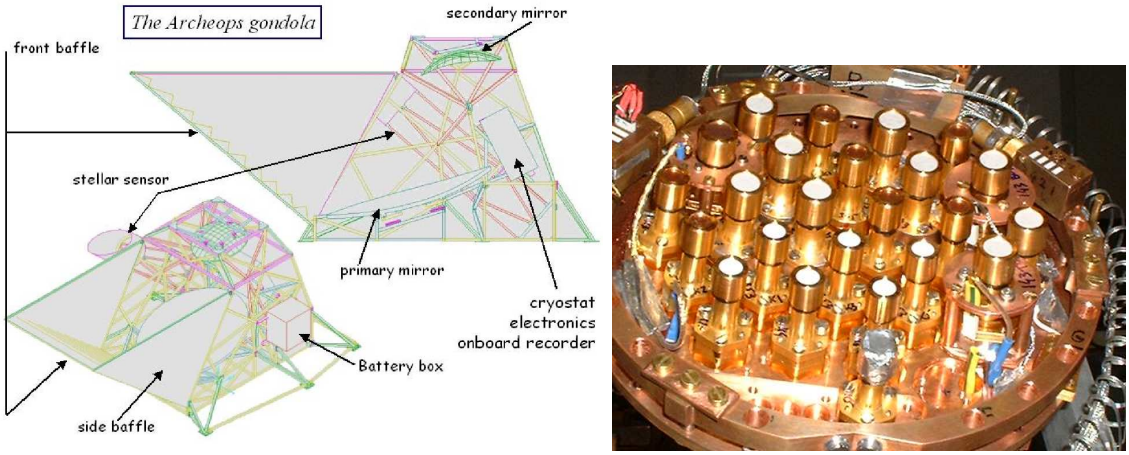

Figure 1: *Left:* Scheme of the ARCHEOPS gondola. *Right:* Picture of ARCHEOPS focal plane.

For high frequency CMB measurements the most important foreground is certainly the emission from Galactic Interstellar Dust (ISD), and few information are available about its polarization properties from the degree to 10 arcmin scale. Measurements are therefore highly required both for Galactic studies of the large scale coherence of the magnetic field and in the field of CMB polarization, but are rather challenging as they require sensitivities comparable to those of CMB studies.

The aim of this paper is to summarize the results obtained by ARCHEOPS on each of these matters. We start by a brief description of the instrument in Sect. 2. Section 3 presents the results on the temperature power spectrum, section 4 gives a summary of the cosmological parameters estimation. Section 5 is dedicated to the results on Galactic dust polarization.

2 Description of the instrument

A detailed description of the instrument technical and inflight performance is given in Benoît *et al* [6,7]. We here focus on essential aspects. The ARCHEOPS telescope is a 1.5 m off–axis Gregorian telescope [25]. In particular, it satisfies the Mizuguchi-Dragone condition [34,20] in which there is negligible cross polarization at the center of the field of view. The detectors are bolometers cooled down to 100 mK by an open cycle ^{3}He–^{4}He dilution cryostat. They operate at frequency bands centered at 143 GHz (8 bolometers), 217 GHz (6), 353 GHz (6=3 polarized pairs) and 545 GHz. The polarization sensitive pairs of bolometers are described in Sect. 5.

Observations are carried out by turning the payload at 2 rpm producing circular scans at a fixed elevation of ~ 41 deg. During a single night, the instrument covers a large fraction of the sky ($\sim 30\%$) as the circular scans drift across the sky due to the rotation of the Earth. This large sky coverage enables to determine the C_ℓ at low multipole values. On the other side, the resolution of the instrument is 13 arcmin on average which therefore enables the determination of the C_ℓ up to high multipoles.

3 Determination of the CMB temperature anisotropies

A more complete discussion is proposed in Benoit *et al* [3]. For the first results of ARCHEOPS on the CMB temperature anisotropies power spectrum [3], we use data from only a single detector at each of the CMB frequencies, 143 and 217 GHz, with a sensitivity of 90 and 150 $\mu K_{CMB}.s^{1/2}$ respectively. To avoid the necessity of detailed modelling of Galactic foregrounds, we restrict the sky coverage to $b > +30$ deg., giving a total of $\sim 100,000$ 15 arcmin. pixels (HEALPIX [21] nside $= 256$) covering 12.6% of the sky (see Fig. 2). To extract the CMB power spectrum, we use the MASTER analysis methodology [23]. We estimate the CMB power

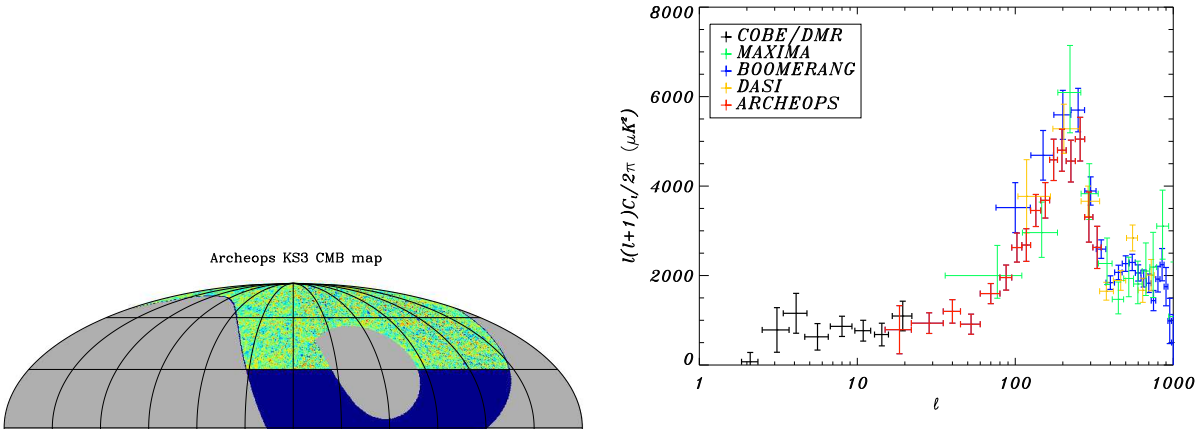

Figure 2: *Left :* ARCHEOPS CMB map (Galactic coordinates, centered on the Galactic anticenter, Northern hemisphere) in HEALPIX pixelisation with 15 arcmin. pixels and a 15 arcmin. Gaussian smoothing. The map is a two–photometers coaddition. The dark blue region is not included in the present analysis because of possible contamination by dust. The colors in the map range from -500 to $500\mu\mathrm{K_{CMB}}$. *Right :* The ARCHEOPS power spectrum compared with results of COBE, Boomerang, Dasi, Maxima.

spectrum in 16 bins ranging from $\ell = 15$ to $\ell = 350$ which can be approximated as independent: off–diagonal terms in the covariance matrix are less than $\sim 12\%$. Sample–variance contributes 50% or more of the total statistical error up to $\ell \sim 200$.

The ARCHEOPS C_ℓ are also computed using two additional independent methods. The first is based on noise estimation with an iterative multi–grid method, MAPCUMBA [16], simple map–making and C_ℓ estimation using SpICE [41] which corrects for mask effects and noise ponderation through a correlation function analysis. The second is based on MIRAGE iterative map–making[44] followed by multi–component spectral matching[11,36,14]. All methods use a different map–making and C_ℓ estimation. Results between the three methods agree within less than one σ.

A comparison of these results with other experiments up to October 2002 (COBE [42], Boomerang [35], Dasi [24], Maxima [32]) is shown in Fig. 2. There is good agreement with other experiments, given calibration uncertainties, and particularly with the power COBE/DMR measures at low ℓ and the location of the first acoustic peak. Work is in progress to improve the cross–calibration of the photometers, the accuracy and the ℓ range of the power spectrum: the low ℓ range will be improved increasing the effective sky area for CMB (which requires an efficient control of dust contamination), the high ℓ range will be improved by including more photometer pixels in the analysis.

4 Estimation of cosmological parameters

A more complete discussion is proposed in Benoit *et al* [4]. Constraints on various cosmological parameters have been derived by using the ARCHEOPS data alone and in combination with other measurements. The ARCHEOPS data give a high signal-to-noise ratio determination of the parameters of the first acoustic peak and of the power spectrum down to COBE scales ($\ell = 15$), because of the large sky coverage that greatly reduces the sample variance.

Cosmological parameter estimation relies upon the knowledge of the likelihood function $\mathcal{L}$ of each band power estimate. Current Monte Carlo methods for the extraction of the C_ℓ naturally provide the distribution function $\mathcal{D}$ of these power estimates. The analytical approach described in [19,1] allows to construct the needed $\mathcal{L}$ in an analytical form from $\mathcal{D}$. Using such an approach was proven to be equivalent to performing a full likelihood analysis on the maps. Furthermore, this leads to unbiased estimates of the cosmological parameters [43,10,18], unlike other commonly used χ^2 methods.

Using ARCHEOPS and COBE data alone and fitting a constant term and a gaussian[28,17], we find (Fig. 3) for the location of the peak $\ell_{\mathrm{peak}} = 220 \pm 6$, for its width $FWHM = 192 \pm 12$,

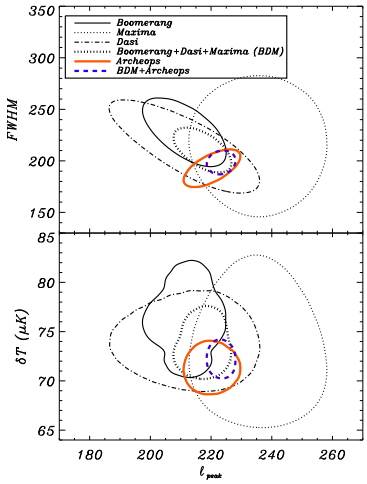

Figure 3: Gaussian fitting of the first acoustic peak using ARCHEOPS and other CMB experiments ($\ell \leq 390$). *Top panel*: 68% CL likelihood contours in the first peak position and FWHM ($\ell_{\rm peak}, FWHM$) plane; *Bottom panel*: 68% CL likelihood contours in the first peak position and height ($\ell_{\rm peak}, \delta T_{\rm peak}$) plane for different CMB experiments and combinations. The width of the peak is constrained differently by ARCHEOPS and BDM experiments, so that the intersection lies on relatively large $\ell_{\rm peak}$. Hence, the BDM + ARCHEOPS zone is skewed to the right in the bottom panel.

and for its amplitude $\delta T = 71.5 \pm 2.0\,\mu$K.

The measured spectrum is in good agreement with that predicted by simple inflation models of scale–free adiabatic peturbations. ARCHEOPS on its own also sets a constraint on open models, $\Omega_{\rm tot} > 0.90$ (68% CL). In combination with COBE [42], DASI [?], BOOMERANG [35], MAXIMA [32], VSA [39], CBI [37] experiments, tight constraints are shown on cosmological parameters like the total density, the spectral index and the baryon content, with values of $\Omega_{\rm tot} = 1.13^{+0.12}_{-0.15}$, $n = 0.96^{+0.03}_{-0.04}$ and $\Omega_{\rm b}h^2 = 0.021^{+0.002}_{-0.003}$ respectively, all at 68% CL and assuming $\tau = 0$. These results lend support to the inflationary paradigm. The addition of non–CMB constraints removes degeneracies between different parameters and allows to achieve a 10% precision on $\Omega_{\rm b}h^2$ and Ω_Λ and better than 5% precision on $\Omega_{\rm tot}$ and n. Flatness of the Universe is confirmed with a high degree of precision: $\Omega_{\rm tot} = 1.00^{+0.03}_{-0.02}$ (ARCHEOPS + other CMB experiments + HST), comparable to that of WMAP [2].

5 First detection of the submillimetre diffuse Galactic dust emission

A more complete discussion can be found in Benoit *et al* [5]. We here complete the introduction to the instrument given in sect. 2 laying the stress on aspects specific to polarization. The polarized channels are assembled in three quasi-optical modules which are equivalent to Ortho Mode Transducers (hereafter OMT [9,13]). The first part of the data processing is common to the channels at 143 and 217 GHz and consists in the removal of the systematics through the pipeline. A specific post–processing is then applied to the 353 GHz channels and aims at removing the remaining low frequency noise without highpass filtering in order not to produce ringing around the Galactic plane. This is achieved through the interpolation of the Galaxy estimated from a SFD template [38] by slowly varying functions [7] and a wavelet shrinkage technique [33] to determine the baseline. Since polarization is obtained from differences of measurements from detectors at various orientations, it is critical that they all be accurately cross–calibrated, typically at the 2% level. This precision is obtained by inter–comparing the

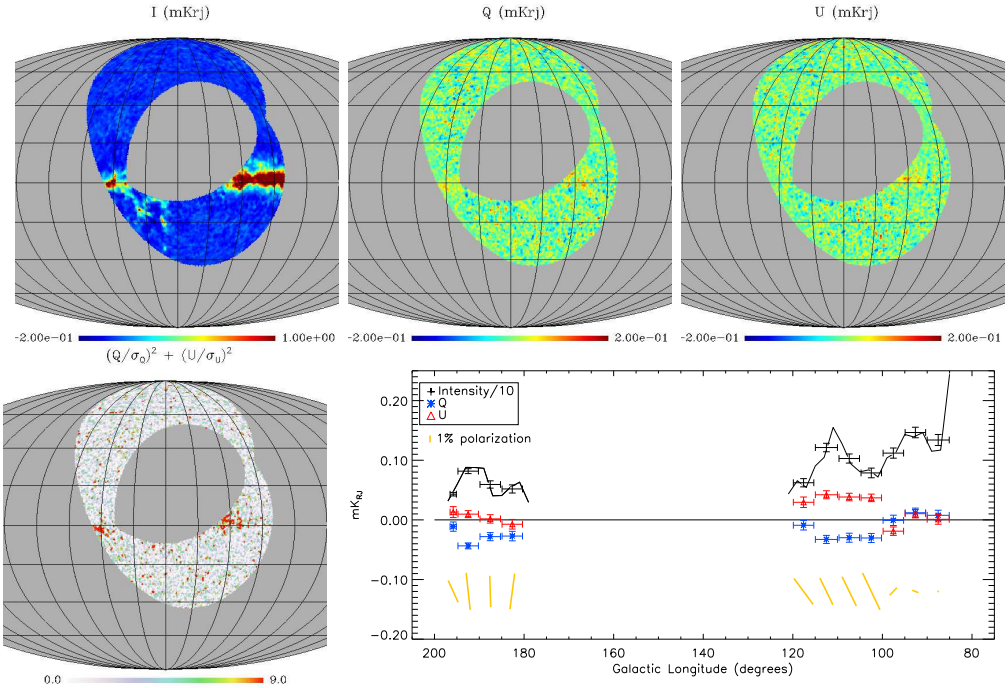

Figure 4: *Top left:* Map of Intensity at 353 GHz. *Top center:* Map of Q Stokes parameter. *Top left:* Map of U Stokes parameter. *Bottom left:* Map of the normalized squared polarized intensity $(Q^2+U^2)/(\sigma_Q^2+\sigma_U^2)$. Twice this quantity is statistically distributed like a χ^2 with 2 degrees of freedom. The 68, 95.4, 99.7% CL of the mapped quantity correspond to 1.1, 3.1, 5.8 respectively. *Bottom right:* Summary figure of diffuse Galactic polarization. The intensity (divided by 10) is represented in black and is taken to be the average value for $-2 \leq b \leq 2$ in each longitude band. The thin solid line is the same value in 2° wide bands. The direction of polarization for every bin is represented below in gold, and the length of the dash is proportionnal to the degree of polarization p in %.

The horizontal error bars represent the width of the longitude bins, which is 5° except for the edge bins.

large signal coming from Galactic "latitude profiles[c]" from different bolometers. Absolute calibration is obtained with respect to FIRAS [31,7].

Once the data are cleaned, calibrated and cross–calibrated, the projection of the Stokes parameters is obtained by forming the linear system $\mathbf{M} = \mathcal{A}\mathbf{S} + \mathbf{N}$, where $\mathbf{M}$ is the time ordered vector of the $n_t \times n_{bol}$ measures, $\mathbf{S}$ the $(3\ n_{pix})$–vector Stokes map of the sky, $\mathcal{A}$ the pointing matrix encoding the pointing information and polarizer angles and $\mathbf{N}$ the $n_t \times n_{bol}$ noise vector. If $\mathcal{N}$ is the noise covariance matrix, the minimum χ^2 solution [26] is:

$$\mathbf{S} = (\mathcal{A}^T \mathcal{N}^{-1} \mathcal{A})^{-1} \mathcal{A}^T \mathcal{N}^{-1} \mathbf{M}. \qquad (1)$$

Solving the linear system (1) is one of the recurrent problems in CMB studies since the matrices and vectors are usually large. In our case, however, the size of the polarized regions correspond to temporal frequencies where the noise is essentially white (in–scan induced noise), and the level of striping in Q and U (cross–scan induced noise) is negligible. We therefore work at low resolution (27 arcmin) and consider each pixel individually. For each pixel, we then compute the (3,3)-matrix $\mathcal{A}^T\mathcal{N}^{-1}\mathcal{A}$ and the (3)-vector $\mathcal{A}^T\mathcal{N}^{-1}\mathbf{M}$. The system of equations thus involves small mathematical objects and the inversion time is small. The resulting maps are presented on Fig. 4.

The emission of two cloud complexes appear to be strongly polarized at 353 GHz. One large complex is in Cassiopeia with an area of 33 deg^2. This area includes the supernova remnant CasA, although the center is detected in the processing as a point source and is not projected. These clouds are polarized up to the 15% level. Systematic uncertainties

[c] A latitude profile is a tabulation of intensity as a function of latitude where the data at all longitudes is averaged to produce a single intensity value in each 2 degrees latitude bin

prevent us from ascertaining the existence of clouds with more than 20%. The other complex coincides with the southern part of Gem OB1. Interestingly, the observed part of the Cygnus complex is not found to be significantly polarized.

In order to study the polarization of the large scale diffuse emission of the dust, we divide the Galaxy into 5 deg wide bands along Galactic longitude and construct for each band three latitude profiles consisting of the values of I, Q and U as a function of latitude. These three profiles are then used to find a unique polarization vector (p, θ) characterizing the region corresponding to the profile. Coherent polarization levels of few percents are significantly detected up to 5 % at the 3 to 4 σ level for several longitude bands, some of which include the clouds already discussed in the previous section. Even after masking these clouds, a significant coherent polarization remains in the same longitude bands. Overall, the orientation is nearly orthogonal to the Galactic plane, compatible with catalogs of starlight polarization[22] and a Galactic magnetic field following the spiral arms. The very low polarization found on Cygnus is in qualitative agreement with this prediction as the spiral arm lies along the line of sight in this longitude range.

A coherence of the orientation of polarization between the diffuse medium and denser clouds is generally observed, except for the cloud G113.2-2.7. It seems that the global magnetic field that pervades the Galactic plane also goes deeply into some denser clouds and is not tangled by turbulence effects. However, the degree of polarization may vary by as much as a factor two inside the same cloud complex. This probably comes from the local variability of the direction of the magnetic field.

Various tests of the possible systematics have been performed, among which the prinipal are different filtering methods of the timelines, different projections of the Stokes parameters, compatibility between the pairs of bolometers, cross–calibration uncertainties, beam effects.

6 Conclusions

If now the results of WMAP [2] have superseded most of the CMB experiments, we whish to remind that ARCHEOPS was the first experiment to estimate the CMB temperature anisotropies power spectrum from the large angular scales of COBE to the entire first acoustic peak. This was obtained with a limited integration time (half a day) using a technology similar to that of the Planck HFI experiment. The measured spectrum is in good agreement with that predicted by simple inflation models of scale–free adiabatic peturbations. The better determination of the first acoustic peak brought by ARCHEOPS improved the accuracy on the cosmological parameters, among which *e.g.* $\Omega_{\rm tot} = 1.00^{+0.03}_{-0.02}$ (ARCHEOPS + CMB + HST).

ARCHEOPS still provides the first large coverage maps of Galactic submm emission with 13 arcmin resolution and polarimetric capabilities at 353 GHz to date. We find that the diffuse emission of the Galactic plane in the observed longitude range is polarized at the 4-5 % level except in the vicinity of the Cygnus region. Its orientation is mostly perpendicular to the Galactic plane and orthogonal, as expected, to the orientation of starlight polarized extinction. Several clouds of few square degrees appear to be polarized at more than 10 %. This suggests a powerful grain alignment mechanism throughout the interstellar medium. Our findings are also compatible with models where a strong coherent magnetic field is coplanar to the Galactic plane and follows the spiral arms, as observed on galaxies[8].

The significant diffuse polarization that we measure indicates that Galactic dust will be a major foreground for future experiments that will study CMB polarization at high frequencies.

1. Bartlett, J. G., Douspis, M., Blanchard, A., & Le Dour, M. 2000, A&AS, 146, 507
2. Bennett, C. L., Halpern, M. Hinshaw, G., *et al.*, 2003 ApJ, submitted, `astro-ph/0302207`
3. Benoît, A., Ade, P., Amblard, A., *et al.* 2003, AA. 399, 25
4. Benoît, A., Ade, P., Amblard, A., *et al.* 2003, AA. 399, 19
5. Benoît, A., Ade, P., Amblard, A., *et al.* 2003, accepted AA
6. Benoît, A., Ade, P., Amblard, A., *et al.*, 2002, Astropart. Phys. 17, 101
7. Benoît, A., Ade, P., Amblard, A., *et al.* 2003, in preparation

8. Berkhuijsen, E. M., Horellou, C., Krause, M., *et al.* 1997, AA, 318, 700, and references therein
9. Bøifot, A. M., Lier, E., Schaug–Pettersen, T., 1990, Proc. Inst. Elect. Eng., 137, 396
10. Bond, J. R., Jaffe, A. H., & Knox, L. 2000, ApJ, 533, 19
11. Cardoso, J. F., Snoussi, H., Delabrouille, J., & Patanchon, G. 2002, Proceed. EUSIPCO02 conf., Toulouse, Sep. 2002, `astro-ph/0209466`
12. Carlstrom, J., To be published in the proceedings of "The Cosmic Microwave Background and its Polarization", New Astronomy Reviews, (eds. S. Hanany and K.A. Olive)
13. Chattopadhyay. G., Carlstrom, J. E., *et al.*, 1999, IEEE microwave and guided wave letters, 9, 339
14. Delabrouille, J., Cardoso, J. F., & Patanchon, G. 2002, MNRAS, submitted, `astro-ph/0211504`
15. de Oliveira-Costa, A., Tegmark, M., Zaldarriaga, M., *et al.*, 2003, Phys.Rev. D67, 023003, `astro-ph/0204021`
16. Doré, O., Teyssier, R., Bouchet, F. R., Vibert, D., Prunet, S. 2001, AA, 374, 358
17. Douspis, M. & Ferreira, P. 2002, Phys. Rev. D, 65, 87302
18. Douspis, M., Bartlett, J. G. & Blanchard, A. & Le Dour, M. 2001a, AA, 368, 1
19. Douspis, M., et al. 2002, A&A, submitted
20. Dragone, C., 1982, IEEE Trans. Ant. Prop., AP-30, No. 3, 331
21. Gorski, K. M. , Hivon, E., Wandelt, B. D.,*et al.* 1998,Proceedings of the MPA/ESO Conferece on Evolution of Large-Scale Structure: from Recombination to Garching 2-7 August 1998; eds. A.J. Banday, R.K. Sheth and L. Da Costa, `astro-ph/9812350`, `http://www.eso.org/science/healpix`
22. Fosalba, P., Lazarian, A., Prunet, S., Tauber, J., 2002, ApJ, 564, 762, and references therein
23. Hivon, E., Gorski, K. M., Netterfield, C. B., et al. 2002, ApJ, 567, 2
24. Halverson, N. W., Leitch, E. M., Pryke, C. et al. 2002, ApJ, 568, 38
25. Hanany, S., & Marrone, D. P. 2002, Applied Optics, 41, 4666
26. Jansen, D. J., Gulkis, S., 1992, "Mapping the Sky With the COBE–DMR", in "The Infrared and Submillimeter Sky after COBE", eds. M. Signore & C. Dupraz (Dordrecht:Kluwer)
27. Keating, B. , O'Dell, C., de Oliveira-Costa, A., *et al.*, 2001, ApJL, 560, L1
28. Knox, L. & Page, L. 2000, Phys.Rev.Lett., 85, 1366
29. Kogut, A., Spergel, D. N., Barnes, C., *et al.*, 2003 ApJ, submitted, `astro-ph/0302213`
30. Kovac, J., Leitch, E. M., Pryke, C., *et al.*, 2002, Nature 420, 772, `astrop-ph/0209478`
31. Lagache, G., 2003, in preparation
32. Lee, A. T., Ade, P., Balbi, A., et al. 2001, ApJL, 561, L1
33. Macías–Pérez, J. F., 2003, in preparation
34. Mizuguchi, Y. , Akagawa, M., & Yokoi, H., 1978, Elect. Comm. in Japan, 61-B, 3, 58
35. Netterfield, C. B., Ade, P. A. R., Bock, J. J., et al. 2002, ApJ, 571, 604
36. Patanchon, G.,et al. 2002, in preparation.
37. Pearson, T. J., Mason, B. S., Readhead, A. C. S., et al. 2002, ApJ, submitted, `astro-ph/0205388`
38. Schlegel, D., Finkbeiner, D., Davis, M., 1998, ApJ, 500, 525
39. Scott, P. F., Carreira, P., Cleary, K., et al. 2002, `astro-ph/0205380`
40. Smoot, G. F., Bennett, C. L., Kogut, A., et al. 1992, ApJ, 396, L1
41. Szapudi, I., Prunet, S., Pogosyan, D., Szalay, A. S., Bond, J. R., et al. 2001, ApJL, 548, L115
42. Tegmark, M. 1996, ApJL, 464, L35
43. Wandelt, B. D., Hivon, E., & Górski, K. M. 2001, PRD, 64, 83003
44. Yvon, D. et al. 2002, in preparation.